Optics Communications 354 (2015) 225–230

Contents lists available at ScienceDirect

Optics Communications

journal homepage: www.elsevier.com/locate/optcom

Electromagnetic scattering by spheres of topological insulators

Lixin Ge [a,b], Dezhuan Han [a,*], Jian Zi [b,c,**]

[a] Department of Applied Physics, Chongqing University, Chongqing 400044, China
[b] Department of Physics, Key laboratory of Micro and Nano Photonic Structures (Ministry of Education), and Key Laboratory of Surface Physics, Fudan University, Shanghai 200433, PR China
[c] Collaborative Innovation Center of Advanced Microstructures, Fudan University, Shanghai 200433, PR China

ARTICLE INFO

Article history:
Received 20 January 2015
Received in revised form
15 April 2015
Accepted 24 May 2015
Available online 4 June 2015

Keywords:
Electromagnetic scattering
Topological magnetoelectric effect
Antiresonance

ABSTRACT

The electromagnetic scattering properties of topological insulator (TI) spheres are systematically studied in this paper. Unconventional backward scattering resulting from the topological magnetoelectric (TME) effect are found in both Rayleigh and Mie scattering regimes. This enhanced backward scattering can be realized by introducing an impedance-matched background. In addition to conventional resonances, interesting antiresonances in scattering coefficients are found in the Mie scattering regime. At the antiresonances, electric or magnetic fields induced by the TME effect can be completely trapped inside TI spheres. In the Rayleigh limit, a method to determine the quantized TME effect of TIs is proposed simply based on the measured electric field components of scattered waves in the far field.

1. Introduction

Topological insulators (TIs) are an emerging quantum phase in condensed matter physics [1–3] with gapless edge or surface states within the bulk energy gap which are protected by time-reversal symmetry. TI materials have been theoretically predicted and experimentally observed in various systems such as HgTe/CdTe quantum well, and $Bi_{1-x}Sb_x$, Bi_2Te_3, Bi_2Se_3 [1,2]. A novel quantized topological magnetoelectric effect (TME) is predicted in TIs: an applied electric field could induce parallel magnetization while an applied magnetic field could induce parallel electric polarization [3]. As a result, an additional term in the Lagrangian $\Delta\mathcal{L} = (\Theta\alpha/4\pi^2)\mathbf{E}\cdot\mathbf{B}$ should be incorporated [3,4], where $\alpha = e^2/\hbar c$ is the fine structure constant, $\Theta = (2p+1)\pi$ is the axion angle with p being an integer, $\mathbf{E}$ is the electric field and $\mathbf{B}$ is the magnetic field. Together with the conventional term in the Lagrangian, it can give a complete description of the electromagnetic (EM) responses of TIs. The corresponding constitutive relations for TIs should be modified as $\mathbf{D} = \varepsilon\mathbf{E} - \bar{\alpha}\mathbf{B}$, $\mathbf{H} = \mathbf{B}/\mu + \bar{\alpha}\mathbf{E}$, where $\mathbf{D}$ and $\mathbf{H}$ are respectively the electric displacement and magnetic field strength, ε and μ are respectively the permittivity and permeability of TIs, $\bar{\alpha} = \Theta\alpha/\pi$ is proportional to the fine structure constant. Indeed, many unusual EM phenomena due to the TME effect have been revealed [5–7].

Scattering of EM waves by small particles is fundamentally interesting with many important applications [8]. Compared with conventional scatterers, scattering of EM waves by scatterers of TIs shows many unusual features due to the presence of the TME effect. For instance, parity-violating scattering under oblique incidence and a strong perturbation of dipole radiations in TI spheres were predicted [9]. Broadband strong scattering in the backward direction and interesting antiresonances were found for TI cylinders [10]. Moreover, the quantization of the TME effect of TI cylinders can even be determined by measuring the electric field components of scattered waves in the far field at one or two scattering angles in the Rayleigh scattering limit [11].

In this paper, we study theoretically scattering of EM waves by spheres of TIs. Based on the standard Mie theory, we derive the scattering coefficients and scattering matrix for TI spheres analytically. Exotic backward scattering due to the TME effect is found in both Rayleigh and Mie scattering regimes, similar to the case for TI cylinders [10]. At certain frequencies, antiresonances of cross-polarized scattering coefficients of TI spheres are revealed, wherein the cross-polarized fields induced by the TME effect are trapped inside TI spheres. In the Rayleigh limit, we propose a simple way to determine the quantized TME effect of TIs by measuring the electric field components of scattered waves in the far field.

2. Mie theory for TI spheres

The system under study is shown in Fig. 1. We consider a TI sphere which is illuminated by a time-harmonic EM wave with an angular frequency ω. The radius of the sphere is a. The dielectric

* Corresponding author.
** Corresponding author at: Department of Physics, Key laboratory of Micro and Nano Photonic Structures (Ministry of Education), and Key Laboratory of Surface Physics, Fudan University, Shanghai 200433, PR China.
E-mail addresses: dzhan@cqu.edu.cn (D. Han), jzi@fudan.edu.cn (J. Zi).

http://dx.doi.org/10.1016/j.optcom.2015.05.054
0030-4018/

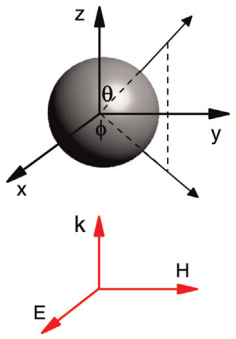

Fig. 1. Schematic view of the system under study. A TI sphere is placed at the origin. An EM plane wave polarized in the x direction is incident along the z direction.

permittivity and magnetic permeability for the TI sphere are (ε_1, μ_1), and those for the background medium are (ε_b, μ_b). The scattering problem can be solved analytically by the standard Mie theory. In the spherical coordinate system, (r, θ, ϕ), the EM fields can be expanded by the vector spherical harmonics [8]: $\mathbf{M}_{e1n}^{(l)}(kr)$, $\mathbf{M}_{o1n}^{(l)}(kr)$, $\mathbf{N}_{e1n}^{(l)}(kr)$ and $\mathbf{N}_{o1n}^{(l)}(kr)$, where subscripts e and o denote respectively the even and odd modes with respect to the x axis, k is the corresponding wavevector ($k_1 = \sqrt{\varepsilon_1\mu_1}\omega/c$ and $k_b = \sqrt{\varepsilon_b\mu_b}\omega/c$ are respectively the wavevectors in the TI sphere and background), n is an integer, and l stands for the kind of the spherical Bessel (Hankel) functions. The incident EM wave can be written as $\mathbf{E}_{inc} = E_0 e^{ik_b z}\hat{\mathbf{e}}_x$, where E_0 is the amplitude. The scattered and internal electric fields can be expanded as follows:

$$\mathbf{E}_{sca} = \sum_{n=1}^{n=\infty} E_n(-b_n\mathbf{M}_{o1n}^{(3)} + ia_n\mathbf{N}_{e1n}^{(3)} - b_n^{\mathrm{TI}}\mathbf{M}_{e1n}^{(3)} + ia_n^{\mathrm{TI}}\mathbf{N}_{o1n}^{(3)}), \tag{1}$$

$$\mathbf{E}_{int} = \sum_{n=1}^{n=\infty} E_n(c_n\mathbf{M}_{o1n}^{(1)} - id_n\mathbf{N}_{e1n}^{(1)} + c_n^{\mathrm{TI}}\mathbf{M}_{e1n}^{(1)} - id_n^{\mathrm{TI}}\mathbf{N}_{o1n}^{(1)}), \tag{2}$$

where $E_n = i^n E_0(2n+1)/n(n+1)$, $\{a_n, b_n\}$ are the conventional scattering coefficients. Different from conventional dielectric spheres, additional terms associated with two new scattering coefficients $\{a_n^{\mathrm{TI}}, b_n^{\mathrm{TI}}\}$, dubbed *cross-polarized* scattering coefficients, arise due to the TME effect. The superscripts 1 and 3 stand for the spherical Bessel function of the first kind and spherical Hankel function of the first kind, respectively. By matching the standard boundary conditions at $r=a$ and applying the modified constitutive relations $\mathbf{D} = \boldsymbol{\varepsilon}\mathbf{E} - \bar{\alpha}\mathbf{B}$, $\mathbf{H} = \mathbf{B}/\mu + \bar{\alpha}\mathbf{E}$ inside the TI sphere, the scattering coefficients a_n, b_n, and the internal coefficients c_n, d_n can be found as

$$a_n = \frac{\mu_b m^2 j_n(mx)[xj_n(x)]'\beta_2 - \mu_1 j_n(x)[mxj_n(mx)]'}{\mu_b m^2 j_n(mx)[xh_n(x)]'\beta_2 - \mu_1 h_n(x)[mxj_n(mx)]'}, \tag{3}$$

$$b_n = \frac{\mu_1 j_n(mx)[xj_n(x)]' - \mu_b j_n(x)[mxj_n(mx)]'\beta_1}{\mu_1 j_n(mx)[xh_n(x)]' - \mu_b h_n(x)[mxj_n(mx)]'\beta_1}, \tag{4}$$

$$c_n = \frac{\mu_1 j_n(x)[xh_n(x)]' - \mu_1 h_n(x)[xj_n(x)]'}{\mu_1 j_n(mx)[xh_n(x)]' - \mu_b h_n(x)[mxj_n(mx)]'\beta_1}, \tag{5}$$

$$d_n = \frac{\mu_1 m j_n(x)[xh_n(x)]' - \mu_1 m h_n(x)[xj_n(x)]'}{\mu_b m^2 j_n(mx)[xh_n(x)]'\beta_2 - \mu_1 h_n(x)[mxj_n(mx)]'}, \tag{6}$$

where j_n and h_n are respectively the spherical Bessel and Hankel functions of the first kind, $x \equiv k_b a$ is the size parameter and $m \equiv \sqrt{\varepsilon_1\mu_1}/\sqrt{\varepsilon_b\mu_b}$ is the relative refractive index. The auxiliary functions β_1 and β_2 are related to the axion angle Θ by $\beta_1 = 1 + \bar{\alpha}^2\chi_1$ and $\beta_2 = 1 - \bar{\alpha}^2\chi_2$, where $\bar{\alpha} = \bar{\alpha}\sqrt{\mu_1/\varepsilon_1}$ and

$$\chi_1 = \frac{\mu_b m^2 j_n(mx)[xh_n(x)]'}{\mu_b m^2 j_n(mx)[xh_n(x)]' - \mu_1 h_n(x)[mxj_n(mx)]'}, \tag{7}$$

$$\chi_2 = \frac{\mu_b h_n(x)[mxj_n(mx)]'}{\mu_1 j_n(mx)[xh_n(x)]' - \mu_b h_n(x)[mxj_n(mx)]'}, \tag{8}$$

The cross-polarized scattering coefficients a_n^{TI} and b_n^{TI}, corresponding to n-th order of electric and magnetic multipoles but with 90° polarization-rotation compared to conventional ones, can be related to the internal coefficients by

$$a_n^{\mathrm{TI}} = -\frac{[mxj_n(mx)]'}{m[xh_n(x)]'}d_n^{\mathrm{TI}}, \quad b_n^{\mathrm{TI}} = -\frac{j_n(mx)}{h_n(x)}c_n^{\mathrm{TI}}. \tag{9}$$

The coefficients c_n^{TI} and d_n^{TI} are the cross-polarized internal coefficients of the TI sphere, related to the normal internal coefficients c_n and d_n by

$$d_n^{\mathrm{TI}} = \bar{\alpha}\chi_1 c_n, \quad c_n^{\mathrm{TI}} = \bar{\alpha}\chi_2 d_n. \tag{10}$$

Obviously, a_n^{TI} (electric) and b_n^{TI} (magnetic) are directly related to the internal multipolar terms c_n (magnetic) and d_n (electric), respectively. This is exactly a manifestation of the TME effect that an applied electric (magnetic) field can induce magnetic (electric) field. For a topologically trivial insulator, the axion angle $\Theta=0$, namely, $\bar{\alpha} = 0$, leading to $\beta_1 = \beta_2 = 1$, $a_n^{\mathrm{TI}} = b_n^{\mathrm{TI}} = c_n^{\mathrm{TI}} = d_n^{\mathrm{TI}} = 0$. The scattering coefficients $\{a_n, b_n\}$ and internal coefficients $\{c_n, d_n\}$ are reduced to be the conventional ones as expected [8].

3. Scattering coefficients in the Rayleigh limit

We assume that both TI and background media under study are non-magnetic, i.e., $\mu_1 = \mu_b = 1$. In the Rayleigh scattering limit ($x \ll 1$ and $mx \ll 1$), it can be shown that only the following scattering coefficients are in the order of x^3:

$$a_1 = -i\frac{2}{3}\frac{3m^2 - 3 + 2\bar{\alpha}^2/\varepsilon_b}{3m^2 + 6 + 2\bar{\alpha}^2/\varepsilon_b}x^3 + O(x^5), \tag{11}$$

$$b_1 = i\frac{2}{3}\frac{\bar{\alpha}^2/\varepsilon_b}{3m^2 + 6 + 2\bar{\alpha}^2/\varepsilon_b}x^3 + O(x^5), \tag{12}$$

$$a_1^{\mathrm{TI}} = b_1^{\mathrm{TI}} = i\frac{2\bar{\alpha}/\sqrt{\varepsilon_b}}{3m^2 + 6 + 2\bar{\alpha}^2/\varepsilon_b}x^3 + O(x^5). \tag{13}$$

All other scattering coefficients are in the order of x^5 or higher and can be hence neglected in the Rayleigh scattering limit. The scattering coefficients a_1 and b_1 correspond to the electric and magnetic dipoles, whereas a_1^{TI} and b_1^{TI} correspond to the cross-polarized electric and magnetic dipoles, respectively.

4. Scattering efficiency

According to the Mie theory, the scattering efficiency for a TI sphere is given by

$$Q_{\mathrm{sca}} = \frac{2}{x^2}\sum_{n=1}^{\infty}(2n+1)(|a_n|^2 + |b_n|^2 + |a_n^{\mathrm{TI}}|^2 + |b_n^{\mathrm{TI}}|^2). \tag{14}$$

Different from conventional dielectric scatterers, the cross-polarized scattering coefficients also contribute to Q_{sca}. Thus, Q_{sca} is dependent on not only the materials parameters ε_1, μ_1, ε_b, μ_b, and x but also the axion angle Θ. We can further decompose Q_{sca} into two terms: the bulk scattering $Q_b = (2/x^2)\sum_{n=1}^{\infty}(2n+1)(|a_n|^2 + |b_n|^2)$ and the scattering caused by surface Hall currents

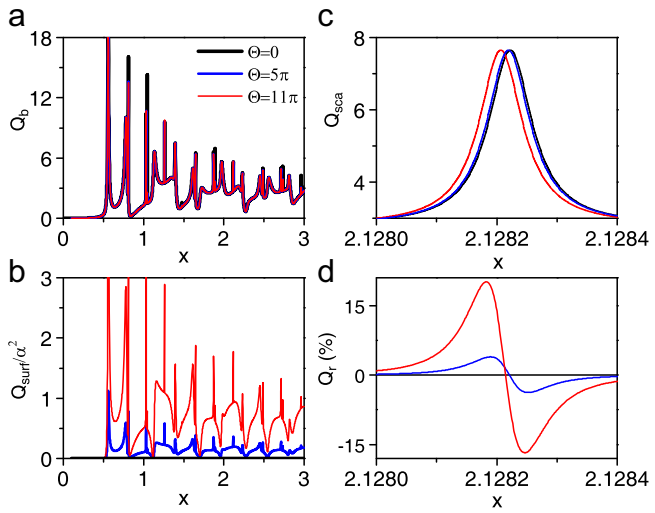

Fig. 2. Scattering efficiency as a function of the size parameter x for different axion angles Θ. (a) Q_b. (b) Q_{surf}. (c) Q_{sca} around the Mie resonance $b_5 = 1$. (d) Relative scattering efficiency Q_r corresponding to the Mie resonance in (c). The dielectric parameters are $\varepsilon_1 = 30$ and $\varepsilon_b = 1$.

$Q_{surf} = (2/x^2)\sum_{n=1}^{\infty}(2n+1)(|a_n^{TI}|^2 + |b_n^{TI}|^2)$. It is obvious that Q_{surf} vanishes as $\Theta = 0$. Note that for the bulk scattering efficiency Q_b it will reduce to the conventional one as $\Theta = 0$.

To estimate the effects of Θ on the scattering efficiency, we take $\varepsilon_b = 1$ (air) as an example. For TI materials, usually $\varepsilon_1 \gg 1$. In the Rayleigh scattering regime, we can obtain an analytical form of the scattering efficiency for TI spheres as

$$Q_{sca} \sim \frac{8}{3}\left[\left(\frac{m^2-1}{m^2+2}\right)^2 + \frac{6m^2}{m^2+2}\left(\frac{\bar{\alpha}}{m^2+2}\right)^2\right]x^4 + O(x^6). \tag{15}$$

The scattering efficiency is proportional to x^4 just as that for conventional dielectric spheres. The difference of Q_{sca} between TI spheres and conventional dielectric ones is an additional term proportional to $\bar{\alpha}^2$.

In the Mie scattering regime, Q_b and Q_{surf} as a function of the size parameter x are plotted in Fig. 2. For different axion angles, Q_b that mainly comes from bulk scattering remains almost unchanged. However, the scattering efficiency Q_{surf} that originates from the surface Hall currents is strongly dependent on the values of the axion angle. For the high-order Mie resonance modes, the contributions from Θ may be clearly observed from the total scattering efficiency, especially near the Mie resonances. In Fig. 2 (c), the peak at $x \simeq 2.1282$ corresponds to the excitation of a magnetic resonant mode with $b_5 = 1$. Compared with that for $\Theta = 0$, the resonance frequency undergoes a red shift [9] for $\Theta \neq 0$. To evaluate the weight of the scattering efficiency contributed from the TME effect, we define a relative scattering efficiency $Q_r = [Q_{sca}(\Theta \neq 0) - Q_{sca}(\Theta = 0)]/Q_{sca}(\Theta = 0)$, shown in Fig. 2(d). As the axion angle Θ increases, Q_r increases as expected. The relative difference of scattering efficiency between $\Theta = 11\pi$ and $\Theta = 0$ can reach almost 20% at the resonant frequency.

5. Unusual backward scattering

Since the wavevector of the incident wave is along the z direction, the scattering direction $\hat{\mathbf{e}}_r$ and the forward direction $\hat{\mathbf{e}}_z$ define a scattering plane. The incident electric fields and the scattered electric fields in the far field ($kr \gg 1$) can be related by a scattering matrix [8]

$$\begin{pmatrix} E_{s\parallel} \\ E_{s\perp} \end{pmatrix} = \frac{ie^{ikr}}{kr}\begin{pmatrix} S_2 & S_3 \\ S_4 & S_1 \end{pmatrix}\begin{pmatrix} E_{i\parallel} \\ E_{i\perp} \end{pmatrix}, \tag{16}$$

where $E_{s\parallel}$ and $E_{s\perp}$ are respectively the components of scattered electric fields parallel and perpendicular to the scattering plane. The corresponding unit vectors parallel and perpendicular to the scattering plane are defined as $\hat{\mathbf{e}}_{s\parallel} = \hat{\mathbf{e}}_\theta$ and $\hat{\mathbf{e}}_{s\perp} = -\hat{\mathbf{e}}_\phi$. The components of incident electric fields parallel and perpendicular to the scattering plane are respectively $E_{i\parallel} = E_0\cos\phi$ and $E_{i\perp} = E_0\sin\phi$, which depend on azimuth angle. The elements of amplitude scattering matrix S_j ($j = 1, 2, 3, 4$) for a single TI sphere are given by $S_1 = \sum_{n=1}^{n=\infty}((2n+1)/n(n+1))(a_n\pi_n + b_n\tau_n)$, $S_2 = \sum_{n=1}^{n=\infty}((2n+1)/n(n+1))(a_n\tau_n + b_n\pi_n)$, $S_3 = \sum_{n=1}^{n=\infty}((2n+1)/n(n+1))(a_n^{TI}\tau_n - b_n^{TI}\pi_n)$, and $S_4 = \sum_{n=1}^{n=\infty}((2n+1)/n(n+1))(b_n^{TI}\tau_n - a_n^{TI}\pi_n)$, where $\pi_n = P_n^1/\sin\theta$ and $\tau_n = dP_n^1/d\theta$ with P_n^1 being the Legendre function. For conventional dielectric spheres, the condition $a_n^{TI} = b_n^{TI} = 0$ leads to a diagonal scattering matrix, i.e., $S_3 = S_4 = 0$. For TI spheres, however, scattering matrix is not diagonal in general since a_n^{TI} and b_n^{TI} may not vanish owing to the TME effect.

With the scattering matrix, the intensity of the scattered waves, defined as energy flux per unit area, can be obtained accordingly. We now discuss the role of the background in the EM scattering. In the Rayleigh limit, only electric and magnetic dipolar terms dominate the EM scattering. The angle-dependent functions π_n and τ_n for $n = 1$ are given by $\pi_1 = 1$ and $\tau_1 = \cos\theta$. Two different limits can be estimated in the following.

(i) For $\varepsilon_1 - \varepsilon_b \gg \bar{\alpha}$, $|a_1| \gg |a_1^{TI}| = |b_1^{TI}| \gg |b_1|$. In other words, the contribution of the conventional electric dipole is much larger than those of the cross-polarized electric and magnetic dipoles induced by TME effect. The intensity of scattered waves is mainly determined by the diagonal terms of the scattering matrix. Thus, the scattering patterns of TI spheres are similar to those of conventional dielectric spheres. In Section 4, the case we discussed with $\varepsilon_1 \gg 1$ obviously satisfies this condition. The bulk scattering still dominate over the scattering from TI surfaces, as shown in Fig. 2.

(ii) For $\varepsilon_1 - \varepsilon_b \ll \bar{\alpha}$, the refractive index of the background is very close to that of the TI sphere. In this case we have $|a_1^{TI}| = |b_1^{TI}| \gg |a_1|$ and $|b_1|$, namely, the conventional electric and magnetic dipoles are negligible compared with the cross-polarized ones. The intensity for the scattered electric field parallel and perpendicular to the scattering plane are respectively given by

$$I_{s\parallel} \simeq \frac{1}{(kr)^2}|S_3|^2\sin^2\phi = \frac{9}{4}\frac{1}{(kr)^2}\left|a_1^{TI}\cos\theta - b_1^{TI}\right|^2\sin^2\phi, \tag{17}$$

$$I_{s\perp} \simeq \frac{1}{(kr)^2}|S_4|^2\cos^2\phi = \frac{9}{4}\frac{1}{(kr)^2}\left|b_1^{TI}\cos\theta - a_1^{TI}\right|^2\cos^2\phi. \tag{18}$$

Here, we assume that the incident plane wave has an unit intensity. Clearly, in the forward direction ($\theta = 0$) the scattered intensity turns to be zero for both $I_{s\parallel}$ and $I_{s\perp}$ since $a_1^{TI} = b_1^{TI}$. In the backward direction ($\theta = \pi$), however, the scattered intensity shows a strong backscattering stemming from the constructive interference of the cross-polarized electric and magnetic dipole radiation, i.e., the terms proportional to a_1^{TI} and b_1^{TI}.

To show these unusual scattering properties, we plot the intensity of scattered waves in the far field for both polarized and unpolarized incident waves in Fig. 3. The dielectric permittivity of TI sphere and background medium are chosen to be $\varepsilon_1 = \varepsilon_b = 30$. The scattering patterns show a strong backward scattering for both Rayleigh and Mie scattering. It is noted that such enhanced or even complete backward scattering has also been found in other systems such as magnetic [12,13], metallic [14], or semiconducting [15,16] particles. For conventional dielectric or metallic spheres, the resonant frequencies for multipoles with different angular

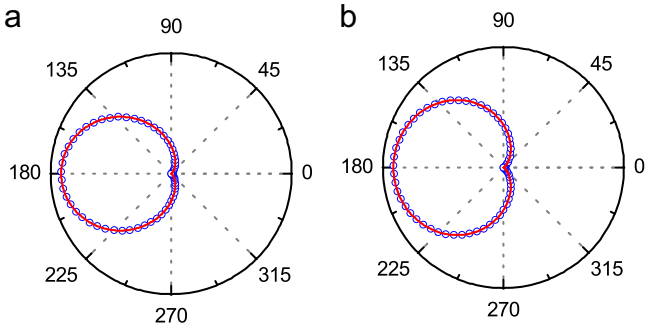

Fig. 3. Intensity of scattered waves for TI spheres in the far field for (a) $x=0.01$ and (b) $x=1$ in the Rayleigh and Mie scattering regimes, respectively. The red lines stand for the incident waves polarized along the x direction while the circles represent unpolarized incident waves. The dielectric constant of the background medium is the same as that of TI spheres. (For interpretation of the references to color in this figure caption, the reader is referred to the web version of this paper.)

momentum channels l are usually different [8,14]. For instance, for an extremely small metallic sphere the resonant frequency for the l-th electric multipole is $\omega_p\sqrt{l/(2l+1)}$, where ω_p is the plasma frequency. However, the enhanced backward scattering here is a broadband effect since the TME effect is a non-resonant phenomenon intrinsically, different from metallic spheres [14] or semiconducting spheres with high refractive index [15,16]. Moreover, the scattering patterns for TI spheres are independent of the polarization of incidents waves as shown in Fig. 3, while for conventional dielectric or metallic spheres the scattering patterns are polarization-dependent.

6. Antiresonances

In Fig. 4, the scattering and internal coefficients corresponding to dipolar modes as a function of the size parameter x are shown. For the scattering coefficients a_1 and b_1, there exist resonances and antiresonances. For instance, the resonances at $x=0.78$ for $|a_1|$ and $x=0.56$ for $|b_1|$ correspond to the excitation of electric and magnetic dipolar modes, respectively. Meanwhile, the internal coefficients d_1 and c_1 have similar resonant behaviors as a_1 and b_1, respectively, indicating that the EM fields inside the sphere have also been strengthened at the corresponding frequencies. In contrast, at the antiresonances ($x=0.835$ for $|a_1|$ or $x=1.06$ for $|b_1|$) no such electric or magnetic dipolar radiation can be detected outside the sphere since the corresponding scattering coefficients vanish at these particular values of x. However, the electric and magnetic dipolar modes still exist inside the sphere since the internal coefficients d_1 and c_1 are actually finite as shown in Fig. 4(c).

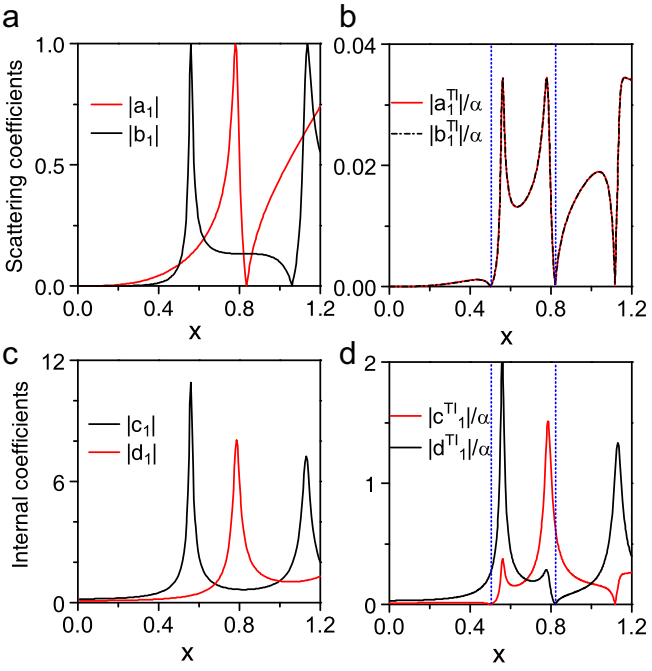

Fig. 4. Scattering and internal coefficients as a function of the size parameter x for $n=1$. The resonant peaks in (a) and (c) mainly come from the bulk scattering. The corresponding size parameter at antiresonances for cross-polarized coefficients are shown by dotted lines in (b) and (d). The dielectric constant of TI spheres is $\varepsilon_1=30$ and the axion angle is chosen to be π. The background is air.

The scattering coefficients a_n and b_n and internal coefficients c_n and d_n for a TI sphere should be similar to those for a dielectric sphere with the same refractive index since the fine structure constant is in the order of 10^{-2}. As a result, the TME effect could not be manifested in the scattering coefficients a_n, b_n and internal coefficients c_n, d_n. However, it plays a key role in the cross-polarized coefficients a_n^{TI}, b_n^{TI} and c_n^{TI}, d_n^{TI} since these four coefficients vanish in conventional dielectric spheres. Interestingly, there also exist resonances and *antiresonances* in a_n^{TI} and b_n^{TI}. At the antiresonances, the cross-polarized scattering coefficients vanish. In order to guarantee $a_n^{\mathrm{TI}}=b_n^{\mathrm{TI}}=0$, the condition $j_n(mx)[mxj_n(mx)]'=0$ should be satisfied. In other words, the antiresonances correspond exactly to the roots of $j_n(mx)=0$ or $[mxj_n(mx)]'=0$. In Fig. 4(b), we take the dipolar mode as an example. The first antiresonance at $x=0.501$ corresponds to $[mxj_1(mx)]'=0$, whereas the second antiresonance at $x=0.82$ corresponds to $j_1(mx)=0$. Although the corresponding scattering fields are zero outside the sphere at the antiresonances, the fields inside the sphere are not necessarily zero. By inspecting the fields inside the TI sphere at $x=0.501$, it is found that cross-polarized electric dipolar mode could be exited since $d_1^{\mathrm{TI}}\neq 0$ whereas cross-polarized magnetic dipolar mode does not exist since $c_1^{\mathrm{TI}}=0$. On the contrary, for $x=0.82$ we have $c_1^{\mathrm{TI}}\neq 0$ and $d_1^{\mathrm{TI}}=0$ as shown in Fig. 4(d), which implies the existence of cross-polarized magnetic dipolar mode and the lack of cross-polarized electric dipolar mode.

From the definition of the vector spherical harmonics [8], the tangential components (i.e., $\hat{\mathbf{e}}_\theta$ and $\hat{\mathbf{e}}_\phi$) of $\mathbf{N}_n$ and $\mathbf{M}_n$ are proportional to $[mxj_n(mx)]'$ and $j_n(mx)$, respectively. Thus, the underlying physics for the existence of anti-resonances of cross-polarized scattering coefficients is that the tangential field components of $\mathbf{N}_n$ or $\mathbf{M}_n$ vanish at the boundary of spheres. Note that the electric (magnetic) fields of electric multipoles are from $\mathbf{N}_n$ ($\mathbf{M}_n$), while those of magnetic multipoles are proportional to $\mathbf{M}_n$ ($\mathbf{N}_n$). In other words, the corresponding tangential field components of the electric and magnetic multipoles should vanish at the boundary. In most cases, the electric and magnetic multipolar fields from the bulk scattering are strong and the cross-polarized ones induced by TME effect cannot manifest themselves. However, the TME effect can be clearly observed at two particular scattering planes, i.e., the planes with $\phi=0°$ and $\phi=90°$. In Fig. 5, we show the field distributions at the scattering plane $\phi=0°$ for the first antiresonance at $x=0.501$ which corresponds to a root of $[mxj_1(mx)]'=0$. The upper panel of Fig. 5 shows the total field distribution. The dominant field components are E_θ and B_ϕ, which are a superposition of the fields from electric dipole (polarized in the x direction) and magnetic dipole (polarized in y direction) modes due to the bulk scattering. The field patterns are almost the same as those for conventional dielectric spheres. Interestingly, the field components E_ϕ and B_θ induced by cross-polarized electric dipole (polarized along the y direction) are nonzero and trapped inside the TI sphere as shown in Fig. 5(c)and (d). The incident and scattered waves do not have these two components (E_ϕ and B_θ) at the scattering plane $\phi=0°$, and the cross-polarized fields induced by

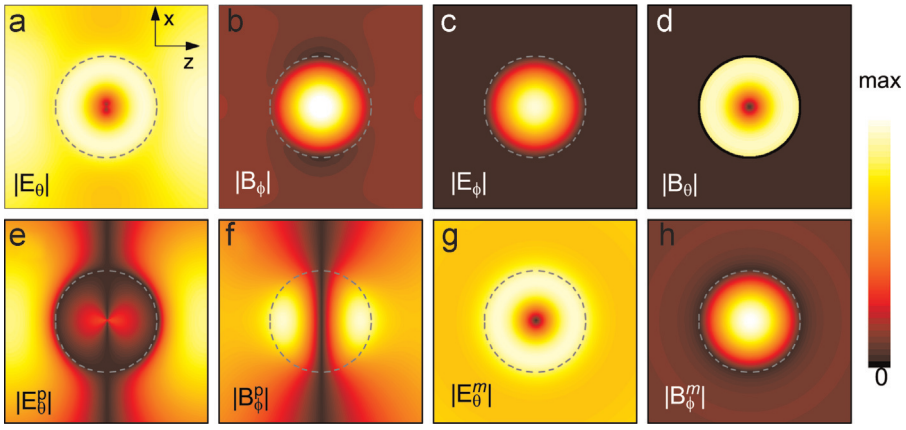

Fig. 5. Distributions of the field components (a) $|E_\theta|$, (b) $|B_\phi|$, (c) $|E_\phi|$, (d) $|B_\theta|$, (e) $|E_\theta^p|$, (f) $|B_\phi^p|$, (g) $|E_\theta^m|$, and (h) $|B_\phi^m|$ in the scattering plane $\phi=0$ at the antiresonance $x=0.501$. The superscripts p and m represent the electric and magnetic dipole terms in the bulk scattering, respectively. The parameters are the same as in Fig. 4. The boundary of the TI sphere is outlined by the dashed lines.

the TME effect are completely trapped inside the sphere. For conventional dielectric spheres [17,18], the scattered waves are basically zero at the antiresonances and thus the spheres become transparent. However, the corresponding field components of incident waves still exist inevitably.

In contrast, at the antiresonances of TI cylinders the electric multipolar modes (corresponding to a_n) and magnetic multipolar modes (corresponding to b_n) due to the bulk scattering can be excited by TE and TM waves, respectively. As is well known, for TI spheres electric multipolar modes (a_n) and magnetic multipolar modes (b_n) can always be excited simultaneously. Therefore, at the antiresonances, the total fields of bulk scattering at the boundary cannot be zero in general. However, the tangential components of the electric and magnetic fields for respectively the electric and magnetic multipolar modes are zero as shown in Fig. 5(e) and (h) for the dipolar case with $[mxj_1(mx)]' = 0$ satisfied. The vanishing of the tangential field components for electric and magnetic multipoles at the antiresonances [10] is an exotic phenomenon and also a strong indication that the TME effect is intrinsically a surface effect. For the second antiresonance at $x=0.82$ similar conclusions can be drawn. The field trapping for the cross-polarized magnetic dipole ($c_n^{\mathrm{TI}} \neq 0$) inside the sphere can also be observed.

7. Determination of the fine structure constant in the Rayleigh limit

A quantitative determination of the TME effect can also be made in TI spheres similar to the case in TI cylinder [11]. We can conduct a Rayleigh-scattering experiment with incident plane waves as shown in Fig. 1. In the far field, both electric-field components of scattered waves $|E_{s\|}|$ and $|E_{s\perp}|$ are measurable quantities and we can thus define a quantity $R(\theta, \phi) = |E_{s\|}|/|E_{s\perp}|$. In the Rayleigh limit, the scattering is dominantly contributed from dipoles. Assuming that $\varepsilon_b = \mu_b = \mu_1 = 1$ we have

$$R(\theta, \phi) = \left| \frac{(\bar{\alpha}^2 - b\cos\theta)\cos\phi - 3\bar{\alpha}(1-\cos\theta)\sin\phi}{(\bar{\alpha}^2\cos\theta - b)\sin\phi - 3\bar{\alpha}(1-\cos\theta)\cos\phi} \right|, \tag{19}$$

where $b = 3m^2 - 3 + 2\bar{\alpha}^2$ can be viewed basically as a bulk parameter. To extract the fine structure constant, we firstly focus on the scattering angles in the first quadrant, i.e. θ and $\phi \in (0, \pi/2)$. Obviously, $\bar{\alpha}^2$ is a small term compared to b, $b\cos\theta$ and hence could be neglected except in the vicinity $\theta \sim \pi/2$. With these assumptions we can obtain

$$\bar{\alpha} = \frac{bR(\theta, \phi)\sin\phi - b\cos\theta\cos\phi}{3(1-\cos\theta)[\sin\phi - R(\theta, \phi)\cos\phi]}. \tag{20}$$

This offers a simple way to determine $\bar{\alpha}$ if $R(\theta, \phi)$ is measured and the parameter m is known. Clearly, this determination of $\bar{\alpha}$ is material-dependent. However, if we set a special observation angle $(\theta, \phi) = (90°, 0°)$, from Eq. (19) $\bar{\alpha}$ is given by

$$\bar{\alpha} = 3R(90°, 0°). \tag{21}$$

Owing to the complete suppression of bulk scattering in this particular angle, the to-be measured $\bar{\alpha}$ now can be solely determined by the value of $R(90°, 0°)$ which is material-independent. From the obtained $\bar{\alpha}$, it offers a way to measure the fine structure constant α since the axion angle is quantized.

8. Conclusions

The EM wave scattering by TI spheres is studied theoretically in a systematic way. The scattering coefficients for TI spheres are derived analytically. In addition to conventional ones, additional terms associated with the TME effect appear. For an impedance-matched background $m \sim 1$, the scattering pattern is highly anisotropic with strong scattering in the backward direction. This strong backscattering or the cancellation of the forward scattering is a manifestation of the TME effect which is basically a surface effect. It can occur in both Mie and Rayleigh scattering regimes and is a broadband effect due to the non-resonant nature of TME effect. The antiresonances found in the Mie scattering regime are another kind of novel phenomena wherein the cross-polarized fields induced by the TME effect are trapped inside the TI spheres. Finally, we propose a simple way to determine the quantized TME effect of TIs in the Rayleigh limit by measuring the electric-field components of scattered waves in the far field.

Acknowledgments

The work is supported by the National Natural Science Foundation of China (Grant no. 11304038) and the Fundamental Research Funds for the Central Universities (Grant no. CQDXWL-2014-Z005). The research of J.Z. is further supported by the 973Program (Grant nos. 2013CB632701 and 2011CB922004).

References

[1] X.L. Qi, S.C. Zhang, Topological insulators and superconductors, Rev. Mod. Phys.

83 (2014) 1057–1110.
[2] M.Z. Hasan, C.L. Kane, Colloquium: topological insulators, Rev. Mod. Phys. 82 (2010) 3045–3067.
[3] X.L. Qi, T.L. Hughes, S.C. Zhang, Topological field theory of time-reversal invariant insulators, Phys. Rev. B. 78 (2008) 195424.
[4] F. Wilczek, Two applications of axion electrodynamics, Phys. Rev. Lett. 58 (1987) 1799.
[5] X.L. Qi, R.D. Li, J.D. Zang, S.C. Zhang, Inducing a magnetic monopole with topological surface states, Science 323 (2009) 1184–1187.
[6] W.K. Tse, A.H. MacDonald, Giant magneto-optical kerr effect and universal faraday effect in thin-film topological insulators, Phys. Rev. Lett. 105 (2010) 057401.
[7] J. Maciejko, X.L. Qi, H.D. Drew, S.C. Zhang, Topological quantization in units of the fine structure constant, Phys. Rev. Lett. 105 (2010) 166803.
[8] C.F. Bohren, D.R. Huffman, Absorption and Scattering of Light by Small Particles, John Wiley and Sons, New York, 1983.
[9] T. Ochiai, Theory of light scattering in axion electrodynamics, J. Phys. Soc. Jpn. 81 (2012) 094401.
[10] L.X. Ge, T.R. Zhan, D.Z. Han, X.H. Liu, J. Zi, Unusual electromagnetic scattering by cylinders of topological insulator, Opt. Express 22 (2014) 30833–30842.
[11] L.X. Ge, T.R. Zhan, D.Z. Han, X.H. Liu, J. Zi, Determination of the quantized topological magneto-electric effect in topological insulators from Rayleigh scattering, Sci. Rep. 5 (2015) 7948.
[12] M. Kerker, D.-S. Wang, C.L. Giles, Electromagnetic scattering by magnetic spheres, J. Opt. Soc. Am. 73 (1983) 765–767.
[13] R.V. Mehta, R. Patel, R. Desai, R.V. Upadhyay, K. Parekh, Experimental evidence of zero forward scattering by magnetic spheres, Phys. Rev. Lett. 96 (2006) 127402.
[14] B.S. Luk`yanchuk, M.I. Tribelsky, Z.B. Wang, M.H.H.Y. Zhou, L.P. Shi, T.C. Chong, Extraordinary scattering diagram for nanoparticles near plasmon resonance frequencies, Appl. Phys. A 89 (2007) 259–264.
[15] Y.H. Fu, A.I. Kuznetsov, A.E. Miroshnichenko, Y.F. Yu, B. Luk'yanchuk, Directional visible light scattering by silicon nanoparticles, Nat. Commun. 4 (2013) 1527.
[16] J.M. Geffrin, B. García-Cámara, R. Gómez-Medina, et al., Magnetic and electric coherence in forward- and back-scattered electromagnetic waves by a single dielectric subwavelength sphere, Nat. Commun. 3 (2012) 1171–1178.
[17] J.A. Schuller, M.L. Brongersma, General properties of dielectric optical antennas, Opt. Express 17 (2009) 24084–24095.
[18] C.W. Hsu, B.G. DeLacy, S.G. Johnson, et al., Theoretical criteria for scattering dark states in nanostructured particles, Nano Lett. 14 (2014) 2783–2788.